Inkjet printed polymer light-emitting devices fabricated by thermal embedding of semiconducting polymer nanospheres in an inert matrix

Evelin Fisslthaler,[1] Stefan Sax,[2] Ullrich Scherf,[3] Gernot Mauthner,[4] Erik Moderegger,[5] Katharina Landfester,[6] and Emil J. W. List[1,a)]
[1]*Institute of Solid State Physics, Graz University of Technology, 8010 Graz, Austria*
[2]*NanoTecCenter Weiz Forschungsgesellschaft mbH, 8160 Weiz, Austria*
[3]*University of Wuppertal, Macromolecular Chemistry, 42119 Wuppertal, Germany*
[4]*Christian Doppler Laboratory Advanced Functional Materials, Institute of Solid State Physics, Graz University of Technology, 8010 Graz, Austria and Institute of Nanostructured Materials and Photonics, JOANNEUM RESEARCH, 8160 Weiz, Austria*
[5]*AT&S Austria Technologie und Systemtechnik AG, A-8700 Leoben, Austria*
[6]*Institute of Organic Chemistry III-Macromolecular Chemistry and Organic Materials, University of Ulm, 89069 Ulm, Germany*

(Received 15 November 2007; accepted 14 April 2008; published online 9 May 2008)

An aqueous dispersion of semiconducting polymer nanospheres was used to fabricate polymer light-emitting devices by inkjet printing in an easy-to-apply process with a minimum feature size of 20 μm. To form the devices, the electroluminescent material was printed on a nonemitting polystyrene matrix layer and embedded by thermal annealing. The process allows the printing of light-emitting thin-film devices without extensive optimization of film homogeneity and thickness of the active layer. Optical micrographs of printed device arrays, electroluminescence emission spectra, and I/V characteristics of printed ITO/PEDOT:PSS/PS/SPN/Al devices are presented.
 [DOI: 10.1063/1.2921780]

The cheap and controlled fabrication of structures on a micrometer and even submicrometer scale is one of the future key issues in micro- and nanoelectronics. The application of semiconducting polymers offers new opportunities for light sources,[1] solar cells,[2] field-effect transistors,[3] and a multitude of other electronic devices as demonstrated over the past decade up to the industrial level. However, for large area applications, such as billboards, there is still a need for low cost and high throughput structured deposition techniques. In particular, for the fabrication of large-scale polymer light emitting diodes (PLEDs), large area uniformity and controlled film thickness, such as achieved by spincasting, have to be combined with printing methods, such as inkjet printing. Despite the fact that inkjet-printed PLEDs have been demonstrated,[4] printing of patterned layers of isolated electroluminescent micrometer-sized areas has up to now only been shown for lithographically prestructured substrates, which also require extensive optimization of film homogeneity and thickness of the active layer.[5] Only recently, one alternative was demonstrated by using a so-called via-hole approach,[6] which combines spincasting with a structuring technique that is based on inkjet printing.

Semiconducting polymer nanospheres[7] (SPNs) provide a convenient alternative approach for the fabrication of printed PLEDs. By means of the miniemulsion process,[8] conjugated polymers that are typically only soluble in organic solvents can be molded into stable water-dispersed colloids with a well-defined particle size. SPNs with diameters that range from a few nanometers to several micrometers[9] can be realized with small size dispersion. As demonstrated for methyl-substituted laddertype poly(*para*-phenylene) (Me-LPPP),[10] such SPNs exhibit unaltered electroluminescence (EL) properties and can be well applied in thin film single and multilayer PLEDs.[11,12] In addition to printing processes, SPNs can be used for assembly techniques such as template assisted self-assembly,[13] directed adsorption,[14] and micromolding in capillaries,[15] allowing for the possibility to structure PLEDs down to a nanometer scale.[16]

SPN dispersions offer good jetting behavior[17] and no bead-on-a-string effect[18] because of the absence of dissolved linear polymer chains with high molecular weight. In addition to environment and user friendliness, such water-based inks also allow for the fabrication of all solution-processed polymer multilayer structures.[12] SPNs dispersed in water can be easily printed on a nonemitting isolating matrix layer deposited from an organic solvent and can be embedded and contacted by thermal treatment to yield large-area light emitting devices with a high pixel resolution down to 20 μm.

A schematic of the device is shown in Fig. 1(a). First, a 40 nm poly(3,4-ethylendioxythiophene)-poly(styrenesulfonate) (PEDOT:PSS) (Baytron P VPAI 4083 from H. C. Starck) and a 40 nm polystyrene (PS) (purchased from Sigma Aldrich, average $M_w \sim 350\,000$) layer were deposited on indium tin oxide (ITO) coated glass. The PS layer was structured by soft embossing[19] using a poly(dimethylsiloxane) stamp with grooves 25 nm deep and 277 nm wide. These grooves ensure a more homogeneous distribution of the SPNs over the printed droplet area. For the printing process, an aqueous dispersion of Me-LPPP SPNs (synthesized as described elsewhere)[8] with a solid content of approximately 0.07 wt % was used. The average diameter of the SPNs was about 100 nm. The aqueous SPN dispersion was inkjet printed[17] by using a Microfab single nozzle printer (nozzle orifice 50 μm), producing drops of approximately 20 μm on the substrate. The printed SPNs were annealed at 140 °C—i.e., well above the glass transition temperature (T_g) of PS (T_g of PS bulk polymer is 95 °C; for very thin

a)Author to whom correspondence should be addressed. Electronic mail: e.list@tugraz.at.

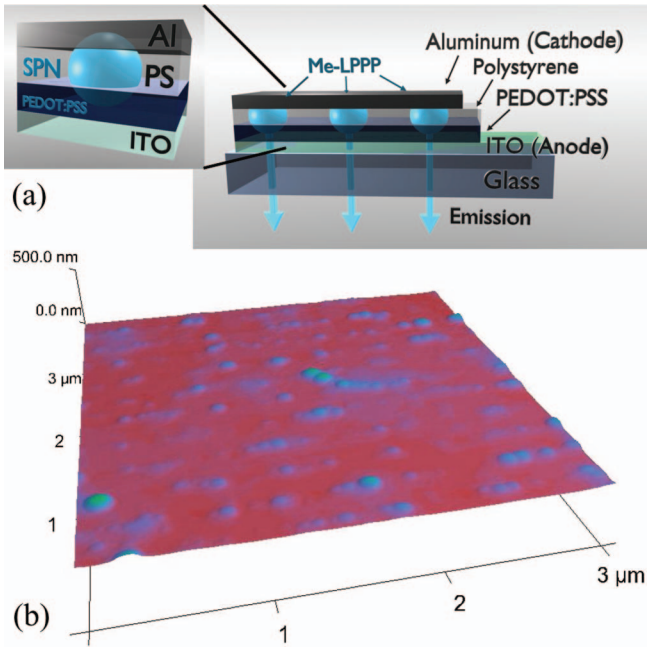

FIG. 1. (Color) (a) Schematic of the assembly of an inkjet-printed SPN polymer light emitting diode, showing the SPNs embedded in the PS layer covered and contacted by a Al top electrode. (b) AFM 3D illustration of an AFM height image, showing the tops of embedded Me-LPPP SPNs protruding from a 80 nm PS layer (Ref. 21).

layers, the T_g is even lower)[20] and well below the T_g of Me-LPPP ($T_g > 300$ °C)[7]—for 12 h. This embedded the SPNs into the PS layer, resulting in good electrical contact with the bottom PEDOT:PSS/ITO electrode.[21] Figure 1(b) shows a three-dimensional (3D) representation of an atomic force microscopy (AFM) height image of the SPNs after the thermal embedding procedure. The SPNs sink into the PS layer but maintain their original spherical shape. Furthermore, it can be seen that the embossed grooves in the PS matrix layer vanish after the thermal treatment and only a certain in-line order of the embedded SPNs can be observed. The layer structure of the device remains unharmed. As a top electrode, aluminum (Al) was evaporated at a base pressure of 5×10^{-6} mbar covering an area of more than 50 individual printed droplets.

Figure 2(a) shows a close-up image of an individual inkjet-printed fluorescing drop recorded with a fluorescence microscope. Figure 2(b) shows the EL emission of two single droplets. Figure 2(c) shows the EL of a droplet array contacted on one device pad. The shape of the dried droplets depicted in Figs. 2(a) and 2(b) shows that the embossed linear grooves in the PS layer not only lead to a linear ordering of SPNs on the nanometer scale [visible in Fig. 1(b)] but also to a slight distortion of the printed droplets so that they are elongated perpendicular to the embossed grooves.

The printing process has been optimized by using different substrate temperatures ranging from 30 to 95 °C to achieve the homogeneous distribution of SPNs and to minimize the formation of a rim as a consequence of the coffee stain effect.[22]

It was found that for substrate temperatures above 70 °C, the fluid evaporates before the drop has had enough time to contract[23] to its equilibrium size after the impact, resulting in a larger spot diameter and not only a less pronounced droplet rim but also a less homogeneous particle

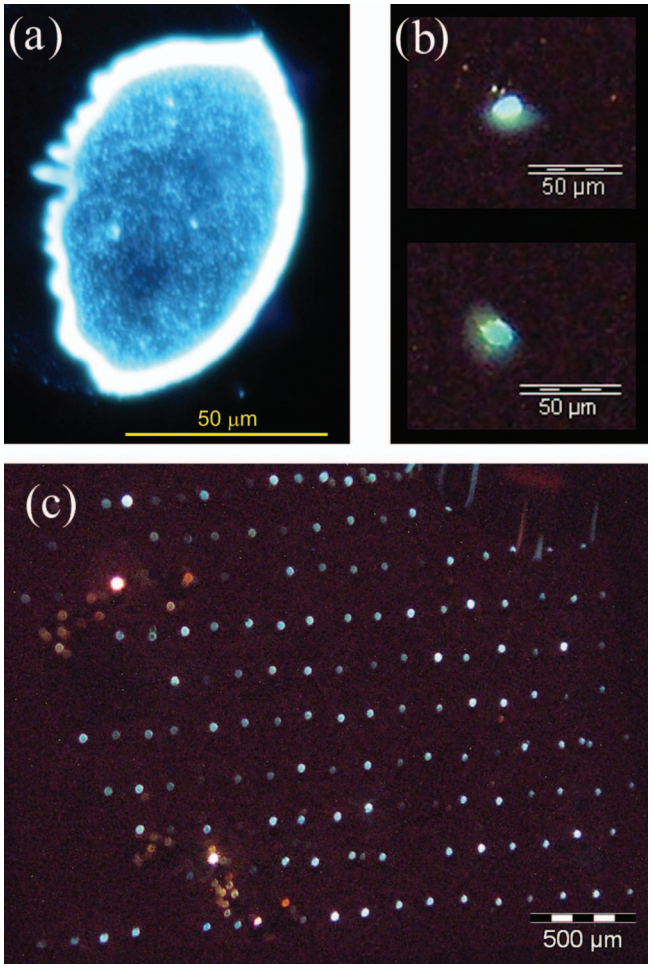

FIG. 2. (Color) (a) Fluorescence microscope image of an inkjet-printed drop of Me-LPPP SPNs picturing the distinctive PL emission from the individual SPNs. (The white emission from the rim is caused by overexposure; the drop is larger than 20 μm due to different printhead parameters.) (b) Close view (optical micrograph) of the EL of two printed spots of Me-LPPP SPNs, showing the bright emission from the interior of the spots (the rim can be seen as a dark ring in the EL pictures.) (c) Optical micrograph of the EL of a whole pad (3×3 mm^2) of an inkjet-printed SPN PLED showing the printed pattern of droplets.

distribution within the drop. The most homogenous light emission of the printed droplets was found for substrate temperatures of 30 °C, which resulted in a uniform spreading of the particles [see Figs. 2(a) and 2(b)]. The droplet rim that is formed due to the coffee stain effect has a width of 5–7 μm for the larger droplets [see Fig. 2(a)] and 1–2 μm for the smaller droplets [see Fig. 2(b)].

Figure 3 shows a current density/voltage (j/V) and a luminescence/voltage (L/V) characteristic of an ITO/PEDOT:PSS/Me-LPPP-SPN/Al PLED device. The current density as well as the luminance has been normalized for the active device area of 3% [see Fig. 2(c), total pad area is 9 mm^2].

For this device, the current onset voltage was measured at approximately 20 V, whereas the EL emission was detectable only above 27 V with the used characterization setup (Ulbricht sphere with source measure unit). This is a consequence of the reduced effective device area. However, the actual luminance onset observable by eye (in the dark) was about the same as the current onset. Above onset, the device reveals a typical rectifying PLED characteristic. Based on an active area of 3%, the total effective luminance can be deter-

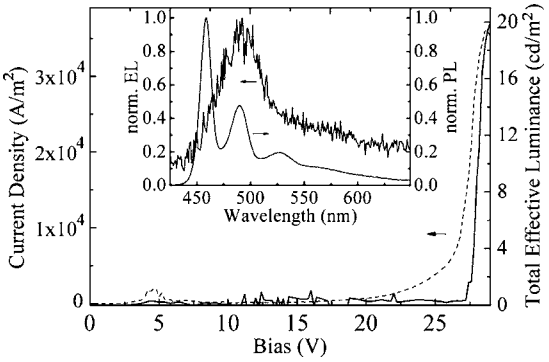

FIG. 3. J/V (dashed line) and L/V (solid line) characteristics of an inkjet-printed Me-LPPP SPN PLED. (Inset) EL spectrum of a Me-LPPP SPN PLED and PL spectrum of a Me-LPPP SPN dispersion.

mined to be at least 20 cd/m^2. Compared to standard spin-coated SPN devices, the printed device shows a large onset voltage, which is attributed to the high work function of aluminum and residue surfactant on the sample surface.

The inset of Fig. 3 shows an EL spectrum of a SPN PLED and a PL spectrum of the SPN dispersion. The PL spectrum matches that of a regular Me-LPPP (Ref. 10) in a thin film with the 0-0 vibronic π^*-π transition at 458 nm and two vibronic bands at 490 and 528 nm. In contrast to the PL spectrum, in the EL spectrum, the 0-0 transition at 458 nm is absent due to self-absorption effects in the active material. Due to the poor electron injection efficiency of the aluminum cathode, the recombination zone is located close to the active material/cathode interface, which leads to the strong self-absorption of the high energy part of the EL spectrum of this low Stokes–Shift polymer.[24]

The approach presented for the micrometer structuring of PLEDs with feature sizes down to 20 μm for isolated electroluminescent spots allows for the facile production of arbitrary light-emitting structures on all scales accessible to inkjet printing based patterning. Future steps will include the further development of the printing process (improvement of patterns) and the optimization of the device structure to achieve enhanced performance.

In comparison to the method presented in Ref. 5, the production method described here is more versatile with respect to printed patterns and utilized active materials. After the embedding, the SPNs are firmly fixed, the deposition of metallic electrode structures from aqueous dispersions by inkjet printing is possible. An additional advantage of the method presented here is that it can be combined with common assembly techniques for colloidal particles, and therefore, offers a route to inkjet printed functional nanostructures.[16]

In conclusion, we succeeded in fabricating 20 μm-PLEDs in a polymer multilayer configuration by inkjet printing an aqueous dispersion of Me-LPPP SPNs onto ITO/PEDOT:PSS/PS substrates with subsequent thermal embedding. This active material is far more environment and user friendly than common polymer solutions that are based on organic solvents, and it is also exceptionally easy to process by printing since it has a very good jetting behavior.

The authors would like to thank Stefan Gamerith, Thomas Piok, Sigi Psutka, and Peter Hadley. The CDL AFM is an important part of the long term AT&S research strategies. This work was performed within the "ISOTEC" project funded by the Austrian NANO initiative (Project DevAna 0706).

[1] R. H. Friend, R. W. Gymer, A. B. Holmes, J. H. Burroughes, R. N. Marks, C. Taliani, D. D. C. Bradley, D. A. Dos Santos, J. L. Brédas, M. Lögdlund, and W. R. Salaneck, Nature (London) **397**, 121 (2000).
[2] N. S. Sariciftci, L. Smilowitz, A. J. Heeger, and F. Wudl, Science **258**, 1474 (1992).
[3] F. Garnier, R. Hajlaoui, A. Yassar, and P. Srivastava, Science **265**, 1684 (1994).
[4] S.-C. Chang, J. Liu, J. Bharathan, Y. Yang, J. Onohara, and J. Kido, Adv. Mater. (Weinheim, Ger.) **11**, 734 (1999).
[5] T. Shimoda, S. Kanbe, H. Kobayashi, S. Seki, H. Kiguchi, I. Yudasaka, M. Kimura, S. Miyashita, R. H. Friend, J. H. Burroughes, and C. R. Towns, Proceedings of the SID 99 Digest (unpublished), p. 376.
[6] Y. Xia and R. H. Friend, Appl. Phys. Lett. **90**, 253513 (2007).
[7] K. Landfester, R. Montenegro, U. Scherf, R. Güntner, U. Asawapirom, S. Patil, D. Neher, and T. Kietzke, Adv. Mater. (Weinheim, Ger.) **14**, 651 (2002).
[8] K. Landfester, Macromol. Rapid Commun. **22**, 896 (2001).
[9] K. Landfester, N. Bechthold, F. Tiarks, and M. Antonietti, Macromolecules **32**, 5222 (1999).
[10] U. Scherf, J. Mater. Chem. **9**, 1853 (1999).
[11] T. Piok, S. Gamerith, C. Gadermaier, H. Plank, F. P. Wenzl, S. Patil, R. Montenegro, T. Kietzke, D. Nehrer, U. Scherf, K. Landfester, and E. J. W. List, Adv. Mater. (Weinheim, Ger.) **15**, 800 (2003).
[12] T. Piok, H. Plank, G. Mauthner, S. Gamerith, C. Gadermaier, F. P. Wenzl, S. Patil, R. Montenegro, M. Bouguettaya, J. R. Reynolds, U. Scherf, K. Landfester, and E. J. W. List, Jpn. J. Appl. Phys., Part 1 **44**, 479 (2005).
[13] Y. Xia, Y. Yin, Y. Lu, and J. McLellan, Adv. Funct. Mater. **13**, 907 (2003).
[14] H. Zheng, I. Lee, M. F. Rubner, and P. T. Hammond, Adv. Mater. (Weinheim, Ger.) **14**, 569 (2002): J. Aizenberg, P. V. Braun, and P. Wiltzius, Phys. Rev. Lett. **84**, 2997 (2000).
[15] H. Li, J.-H. Zhu, J.X. Shi, and P.-S. He, Chin. J. Chem. Phys. **19**, 352 (2006).
[16] E. Fisslthaler (unpublished).
[17] G. Mauthner, K. Landfester, A. Köck, H. Brückl, M. Kast, C. Stepper, and E. J. W. List, Org. Electron. **9**, 164 (2008).
[18] R. P. Mun, J. A. Byars, and D. V. Boger, J. Non-Newtonian Fluid Mech. **74**, 285 (1998).
[19] M. Geissler and Y. Xia, Adv. Mater. (Weinheim, Ger.) **16**, 1249 (2004); Y. Xia and G. M. Whitesides, Annu. Rev. Mater. Sci. **28**, 153 (1998); J. Narasimhan and I. Papautsky, J. Micromech. Microeng. **14**, 96 (2004).
[20] J. A. Forrest and K. Dalnoki-Veress, Adv. Colloid Interface Sci. **94**, 167 (2001).
[21] See EPAPS Document No. E-APPLAB-92-022819 for additional information. For more information on EPAPS, see http://www.aip.org/pubservs/epaps.html.
[22] R. D. Deegan, O. Bakajin, T. F. Dupont, G. Huber, S. R. Nagel, and T. A. Witten, Nature (London) **389**, 827 (1997).
[23] H. Dong, W. W. Carr, and D. G. Bucknall, AIChE J. **53**, 2606 (2007).
[24] F. P. Wenzl, P. Pachler, E. J. W. List, D. Somitsch, P. Knoll, S. Patil, R. Guentner, U. Scherf, and G. Leising, Physica E (Amsterdam) **13**, 1251 (2002).